Evaluation of SPOT HRV-XS Data for Kelp Resource Inventories

Eric W. Augenstein, Douglas A. Stow, and *Allen S. Hope*
Department of Geography, San Diego State University, San Diego, CA 92182

ABSTRACT: Digital multispectral images acquired from the SPOT High Resolution Visible (HRV) satellite system were evaluated for their use in mapping the distribution and quantifying the abundance of giant kelp (*Macrocystis pyrifera*) resources off the coast of San Diego, California. Analysis of spectral radiance data acquired from SPOT satellite and boat platforms revealed that higher values in the near infrared band (XS3) corresponded to areas where the kelp surface canopy had a higher density. Bands XS2 (red) and XS1 (green) were marginally useful for discriminating kelp from open water, but these bands were useful for minimizing confusion between kelp and turbid nearshore water that occurred in the NIR band. Spatial distributions of kelp derived from SPOT XS3/XS2 (NIR/red) band ratio images closely corresponded to distributions derived from color infrared (CIR) aerial photographs. SPOT HRV-XS digital data can be processed to yield kelp survey maps that fulfill the resolution and accuracy requirements of most resource mapping and monitoring applications. The primary advantages of these data over CIR aerial photography are the ability to map several relative levels (or classes) of kelp density directly and to derive estimates of kelp areal extent in a more repeatable manner.

INTRODUCTION

THE ECOLOGICAL IMPORTANCE of kelp beds and the growing demand for seaweed as an industrial raw material make it increasingly important to gather accurate and complete data on the location, abundance, and harvest potential of kelp resources (Austin and Adams, 1978). The effective, long-term management of coastal kelp resources requires accurate maps of the spatial distributions of kelp canopy and consistent estimates of the kelp's areal extent. Kelp canopy distribution maps are traditionally derived by manual interpretation of color infrared (CIR) aerial photographs (N. M. I., 1981). Manually derived estimates of kelp areal extent often vary greatly depending upon the interpreter and cartometric method used (N. M. I., 1981), and maps of canopy change between dates and quantitative measures of canopy density are difficult to produce (W. North, personal communication, 1989).

Data from imaging spectral radiometers mounted on aircraft or satellites can be digitally processed to yield information on kelp distributions more efficiently than by manual interpretation of aerial photographs. Multi-temporal satellite imagery can provide a synoptic database from which to evaluate macroscale changes in kelp populations over large areas of coastline, as well as smaller scale fluctuations within individual kelp beds. In two previous studies by Jensen *et al.* (1976; 1980), the utility of Landsat multispectral scanner (MSS) imagery and digital classification methods was analyzed for mapping and estimating the areal extent of kelp beds off the coast of Santa Barbara, California. The Landsat MSS estimates of areal extent were highly correlated with estimates derived from aerial photographs; however, the kelp extent was underestimated (mostly due to the limited spatial and radiometric resolution of the Landsat MSS). A subsequent study by Jensen *et al.* (1987) used a time sequence of Landsat MSS, Thematic Mapper (TM), and aircraft Thematic Mapper Simulated (TMS) digital data to document changes in giant kelp distribution for two Santa Barbara beds.

The objective of this study was to evaluate the utility of digital multispectral (XS) radiance data acquired from the High Resolution Visible (HRV) sensor of the Systeme Probatoire d'Observation de la Terre (SPOT) satellite system for mapping the distribution and abundance of kelp resources. The SPOT HRV, with its nominal 20-metre resolution in XS mode, should be appropriate for resolving detailed attributes of kelp beds, while covering as much as 85 km of coastline. Although the focus of this investigation was to evaluate the utility of the data acquired by satellite, *in situ* observations using a portable radiometer were also used to determine the spectral radiance and reflectance characteristics of the kelp canopy at the sea surface. The reflected spectral radiance measurements acquired from both SPOT satellite and boat platforms were used to determine the optimum SPOT HRV bands for the discrimination of kelp, and to determine how the spectral signature of kelp varies with its abundance at the sea surface. Image processing techniques were applied to the SPOT HRV digital data for mapping the areal extent and density of the kelp canopy, and their temporal changes.

BACKGROUND AND STUDY AREAS

Macrocystis pyrifera (giant brown kelp) is a species of seaweed that is noteworthy for its commercial value as a renewable natural resource and its ecological importance as a marine habitat (North, 1971). Undersea forests of giant kelp occur in many temperate waters of the world, but are especially well developed off the coast of California from San Diego to Monterey (McPeak and Glantz, 1984). *Macrocystis* forms a buoyant canopy at the sea surface which can become extremely dense when mature, thus making it well suited to aerial inventory techniques (Mel, 1977). Kelp forests support a variety of commercial and sport fisheries along the California coast, and serve as habitat for hundreds of species of marine life (North, 1971). Kelp has also been harvested commercially since the early 1900s. Modern techniques use barges with rotating blades to harvest the surface canopy to a depth of one metre below the water line, which leaves the subsurface ecosystem relatively undisturbed (McPeak and Glantz, 1984). Kelp's most important use is as the primary source of algin, a natural compound with a special ability to control the properties of mixtures containing water, which is used in a wide variety of products and manufacturing processes (McPeak and Glantz, 1984).

Kelp populations are subject to extreme fluctuations due to environmental factors that include storm events, water temperature changes, low nutrient levels, predation (primarily by sea urchins), and pollution (N. M. I., 1981). Kelp distribution maps and estimates of areal extent are important sources of information for kelp harvesting companies, marine biologists, and public agencies such as the Department of Fish and Game, National Park Service, and San Diego Regional Water Quality Control Board. The maps are used to document changes in kelp distribution over time and to pinpoint problem areas for subsequent investigation by boat and diving surveys. Kelp maps

PHOTOGRAMMETRIC ENGINEERING & REMOTE SENSING,
Vol. 57, No. 5, May 1991, pp. 501–509.

0099-1112/91/5705–501$03.00/0

are currently produced by mosaicking CIR aerial photographs and manually tracing the boundaries and density patterns of each bed onto a base map (N. M. I., 1981). Estimates of aerial extent are usually derived by planimeter or the grid count method. Both of these cartometric methods are subject to several sources of interpreter and instrument error (Maling, 1989). Different photo-interpreters often use different criteria for defining the boundary of a kelp bed, and differences of 50 to 200 percent have have observed when comparing areal extent estimates of the same bed derived by two or more sources (N. M. I., 1981).

The La Jolla and Point Loma kelp beds off the coast of the San Diego, California area were selected as study sites for this project (Figure 1). The La Jolla bed was chosen as the primary study site because its geographic area was encompassed by both SPOT scenes used in this study, while the southern portion of the Point Loma bed was not covered in the earlier (1986) image. During the 1986 to 1987 time frame of this study, the Point Loma and La Jolla beds were, respectively, the largest and second largest kelp beds off the southern California coast, covering their greatest extents since the early 1950s (R. McPeak, personal communication, 1988). Along the coastal study areas, *M. pyrifera* commonly grows in water depths ranging from 5 to 20 metres (Mel, 1977) which occurs between 150 and 2000 metres from the shore.

METHODOLOGY

Data Acquisition

The primary sources of data used for this study were SPOT HRV-XS digital data acquired on two dates, and spectral radiometer measurements of kelp beds acquired from a boat. In addition, new and existing aerial photography of the kelp beds were acquired and used for comparison with kelp distributions derived from the SPOT HRV-XS data. Collateral data on ocean conditions were also obtained for each acquisition date.

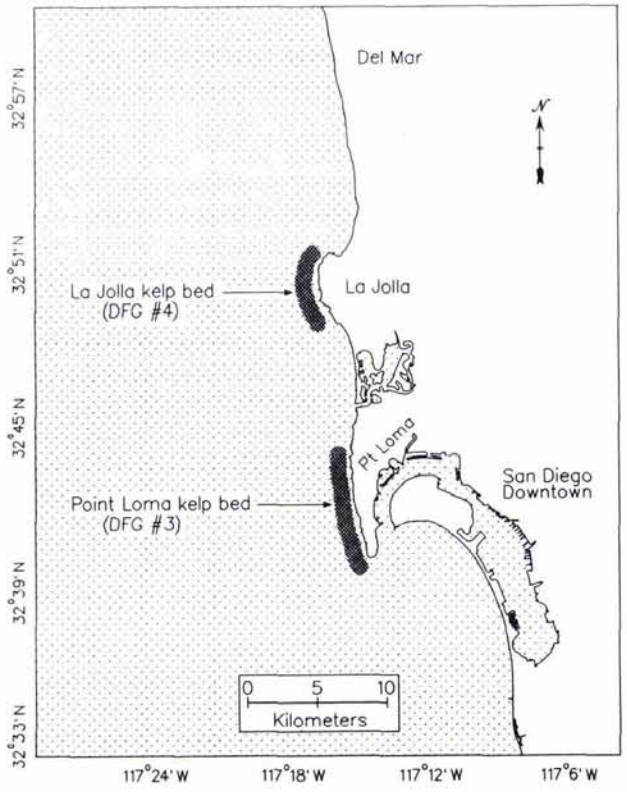

FIG. 1. Location of the La Jolla and Point Loma Kelp bed study sites in the San Diego, California area. California Department of Fish and Game (DFG) designation numbers for each bed are also indicated.

Spectral radiance data were acquired from boat over kelp and open water on 23 August 1987 between 1130 and 1240 PDT using a portable Exotech radiometer mounted on a boom. The four channels of the radiometer were configured with spectral filters to sense reflected radiance in the wavebands corresponding to the SPOT HRV-XS sensor and band 1 of the Landsat Thematic Mapper (TM):

- Landsat TM1 0.45 to .52μm (blue-green)
- SPOT HRV-XS1 0.50 to 0.59μm (green)
- SPOT HRV-XS2 0.61 to 0.68μm (red)
- SPOT HRV-XS3 0.79 to 0.89μm (near infrared)

At the sensor height of 1.5 metres above the sea surface, the 15° IFOV provided a radiometer footprint, or spatial resolution, of approximately 0.40 metres (a circular area of approximately 0.13 m^2). Spectral radiance was sampled over areas of the La Jolla kelp bed that were visually stratified into high, medium, or low density classes, as well as over open water containing no kelp, both within and outside the kelp bed. The term "density" refers to an *in situ* visual assessment of the amount or proportional coverage of surface kelp present within the sampling area relative to other parts of the bed. Quantitative density measurements are usually derived from diving surveys and could not be obtained within the scope of this study. Thirty-five millimetre (35-mm) photographs of sample areas were acquired along with radiometer samples to verify the *in situ* surface coverage estimates. Subsequent analysis of these photographs revealed that the proportion of kelp in low density sample areas ranged from approximately 0 to 35 percent, medium density samples 25 to 75 percent, and high density samples 50 to 95 percent. Spectral radiance data were also acquired over a diffuse reflector panel with a surface coating of barium sulfate ($BaSO_4$) one hour before and one hour after the acquisition of the kelp bed radiometer samples (the hour being travel time between kelp bed and harbor). These data were later used as calibration factors to derive spectral reflectance from spectral radiance measurements.

Color and CIR aerial photos of the La Jolla kelp bed were obtained from archives, and new 35-mm CIR slides were photographed obliquely from a light aircraft. Kelp distribution maps of La Jolla and Point Loma derived from CIR aerial photographs were also obtained (W. North, unpublished maps, 1986-1987).

Two SPOT HRV-XS images of the San Diego area (SPOT Grid Reference System K544/J284) were obtained. Acquisition parameters and ocean conditions data for each scene are shown in Table 1. The digital tapes were pre-processed to level 1B, which includes equalization of detector responses and corrections for systematic geometric distortions (SPOT Image Corporation, 1989).

Image and Radiometric Data Processing

Subscenes of the La Jolla kelp bed area were extracted from both SPOT HRV-XS images, and an additional subscene of the Point Loma kelp bed was extracted from the 1987 image. Spectral signatures were derived for pixels within sample sites representing three kelp density classes (low, medium, and high density), open ocean beyond the bed, and nearshore ocean between the bed and coastline. The selection of low, medium, and high density sample sites was based on the density (or spacing) of the kelp canopy interpreted from CIR aerial photographs of the La Jolla bed and maps derived from the aerial photographs (W. North, unpublished maps, 1986 and 1987). Brightness value (BV) means and ranges for each sample class were then evaluated to determine the BV ranges for the three kelp classes and two ocean classes in each of the three SPOT HRV-XS bands.

TABLE 1. SPOT SCENE PARAMETERS AND OCEAN CONDITIONS

	22 Nov 86	10 Oct 87
Time of Scene Center:	18:38:14 GMT	18:45:35 GMT
Location of Scene Center:	N 32° 54'59" W 117° 00'23"	N 32° 38'47" W 117° 02'45"
Along-Track Orientation:	10.1°	11.0°
Sensor Incidence Angle:	4.3° right/East	9.7° left/West
Solar Azimuth:	63.8°	61.0°
Solar Elevation:	35.6°	49.1°
Onboard Gain Numbers:	XS1 & XS3 = 5, XS2 = 6	XS1 & XS3 = 5, XS2 = 6
Absolute Calib. Gains:	XS1 = 0.92845 XS2 = 0.67688 XS3 = 0.95082	XS1 = 0.86195 XS2 = 0.89631 XS3 = 0.90817
Tide Height (m)[a]	0.7	1.9
Wave Height (m)[b]	1.2–1.6	0.5–0.75
Wind Speed (kt)[c]	10–11	7–8

[a] U. S. Department of Commerce, National Oceanic and Atmospheric Administration, National Ocean Service, 1986 and 1987
[b] U. S. Army Corps of Engineers and State of California, Department of Boating and Waterways, 1986 and 1987
[c] National Weather Service, San Diego, Calif.

The spectral signatures for sample sites indicated that some areas of low density kelp and turbid nearshore water were radiometrically similar in the near infrared (NIR) band (XS3), but were separable in the red (XS2) and green (XS1) bands. Confusion between kelp and turbid water areas in the NIR could therefore be reduced by incorporating information in the red or green bands. Based on these findings, image ratios of the NIR divided by the red (XS3/XS2) and NIR divided by the green (XS3/XS1) were computed from the image BVs. Thresholds for recoding ratio values into low, medium, and high density kelp classes and water were determined from the sample site signatures and applied to the ratio images.

The two SPOT scenes were registered using a "rubber sheeting" method for subsequent change detection processing. Shoreline and inland cultural features were selected as ground control points (GCPs) from both images. The 1987 image was registered to the 1986 image using a first-order image transformation based on these GCPs and nearest neighbor resampling. The image data in the two registered scenes were then radiometrically normalized (by means of histogram adjustments to the 1987 image BVs) to partially compensate for differences in sensor incidence angle and differences in illumination between the two dates.

Several image change detection algorithms were then applied, including differencing, overlay, ratioing, and unsupervised clustering using the two SPOT images to produce maps of kelp canopy change. The XS3/XS2 ratio images from both dates were also classified to create thematic maps in raster format. Pixels were grouped into ocean or kelp classes according to threshold values derived from the multispectral sample sites. Land areas were visually delineated and masked from further processing. The resultant kelp/ocean thematic maps from both dates (in raster format) were then combined by recoding them into a third map, sometimes called a "matrix" GIS analysis technique (Jensen, 1986). The resultant thematic map identified transition categories (i.e., gain, loss, or no change in canopy coverage between dates).

To estimate kelp areal extent from the SPOT HRV-XS data, subscenes from XS3/XS2 ratio images containing only the kelp bed and surrounding ocean areas were extracted for the La Jolla bed in 1986 and 1987 and Point Loma bed in 1987. The number of pixels in each subscene with XS3/XS2 ratio values above the class threshold for low density kelp were totaled. These totals were then multiplied by a factor of 400 (the nominal ground area in square metres covered by a SPOT HRV-XS pixel) to estimate the areal extent of the kelp bed in square metres.

Spectral radiometer data from boat and SPOT platforms were converted to units of spectral radiant exitance (SRE) for subsequent analysis of the appropriateness of the SPOT HRV-XS spectral bands for kelp discrimination. Radiometer measured voltages acquired from boat were converted to SRE measured in watts per square metre (Wm^{-2}). SRE data acquired from boat were also converted to units of spectral reflectance by dividing the kelp bed SRE values by SRE values acquired over the diffuse reflectance panel. The histogram-adjusted SPOT BVs were transformed into SRE values by first deriving equivalent radiance using the SPOT calibration gain coefficients supplied on the digital tapes (see Table 1), and then converting to SRE [Wm^{-2}] by assuming isotropic reflectance (Singh, 1985).

Three commonly used spectral vegetation indices were applied to the spectral radiant exitance data sets, including (1) the simple ratio (SR or NIR/Red), (2) the normalized difference vegetation index (NDVI), and (3) the transformed vegetation index (TVI). A near infrared divided by green ratio was also tested, because kelp was shown by Jensen et al. (1980) to reflect more incident red radiation than green.

RESULTS AND DISCUSSION

SPECTRAL-RADIOMETRIC CHARACTERISTICS OF KELP

The spectral radiant exitance (SRE) and spectral reflectance data acquired from a boat are summarized in Table 2, and the mean SRE and reflectance values in the four bands for each sample class are shown graphically in Figures 2a and 2b, respectively. The nearshore ocean water contained some suspended sediment and had a rough surface during sampling, resulting in peak SRE and reflectance in the green band (XS1) and lowest values in the NIR band (XS3). High variance in SRE and reflectance for all four bands was attributed to a large amount of specular reflectance of the incident energy (i.e., sun glint) by facets of the rough water surface. The higher SRE means in general compared to clear, calm ocean were caused by substantial amounts of suspended sediment, as well as the sun glint factor described previously. In contrast, measurements acquired over very clear, calm water within a clearing in the center of the bed exhibited lower mean and standard deviation in all four bands, with peak SRE occurring in the blue-green (TM1).

Low density kelp plots were sampled in patchy, outer portions of the bed where a large percentage of the kelp remained a few centimetres below the sea surface. SRE and reflectance for low density plots was similar to that for clear water (especially in the blue-green and green bands), showing that the low density areas were dominated by ocean spectral characteristics. Medium density plots were sampled in thicker areas of the bed where the kelp fronds rose slightly above the sea surface, and the high density plots were sampled in areas with a dense, fully developed surface canopy. Spectral reflectance characteristics of the high density plots were dominated by emergent kelp, and SRE and reflectance in the NIR band (XS3) were found to increase in proportion to the surface density of the kelp canopy. Analysis of the spectral reflectance data showed that kelp reflects equal or higher percentages of incoming red radiation than green radiation (which causes *M. pyrifera* to appear brownish in color). In contrast, SRE for kelp was higher in the green than red waveband due to greater incoming green radiation.

A coincident spectral plot of the boat spectral radiant exitance data is shown in Figure 3. The range of SRE in band XS3 was distinctly different for the three kelp classes, but overlap occurred between low density (and some medium density) kelp

TABLE 2. SPECTRAL RADIANT EXITANCE (SRE) [Wm^{-2}] AND SPECTRAL REFLECTANCE (%) MEAN AND STANDARD DEVIATIONS FOR FIVE CLASSES OF DATA ACQUIRED FROM BOAT

		TM1—(bl-grn)				XS1—(green)				XS2—(red)				XS3—(NIR)			
Class	n	Mean SRE	S.D. SRE	Mean Ref.	S.D. Ref.	Mean SRE	S.D. SRE	Mean Ref.	S.D. Ref.	Mean SRE	S.D. SRE	Mean Ref.	S.D. Ref.	Mean SRE.	S.D. SRE	Mean Ref.	S.D. Ref.
Nearshore Ocean	41	3.15	1.87	2.62	1.42	4.08	3.73	3.37	2.73	2.38	3.29	2.56	2.77	1.66	2.15	2.13	2.35
Clear Ocean	10	1.92	0.88	1.52	0.69	1.67	0.59	1.27	0.45	0.77	0.38	0.79	0.38	0.27	0.06	0.29	0.04
Low Density Kelp	50	1.84	1.92	1.48	0.83	2.01	1.25	1.57	0.73	1.49	1.65	1.54	1.23	1.08	1.23	1.28	1.39
Medium Density Kelp	49	1.27	0.58	1.06	0.30	1.92	0.89	1.55	0.52	1.45	0.61	1.57	0.48	3.42	2.47	4.42	1.71
High Density Kelp	80	1.66	0.87	1.34	0.56	2.39	1.02	1.87	0.63	2.21	1.02	2.31	0.91	6.24	2.86	7.61	2.12

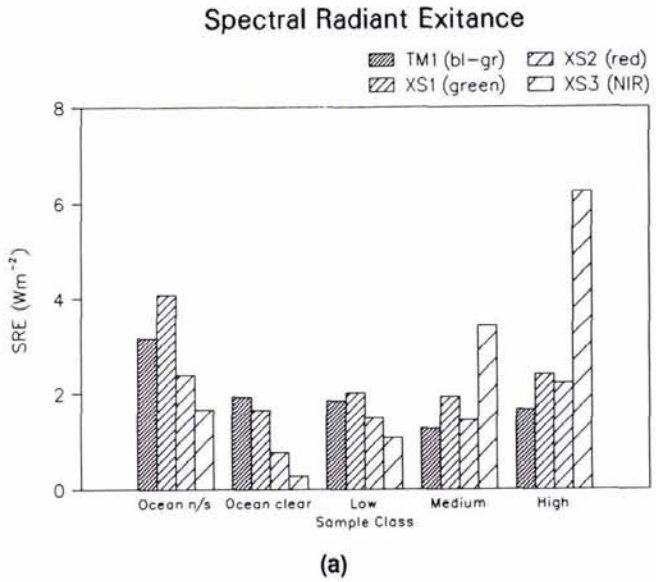

FIG. 2. Mean spectral radiant exitance (a) and mean spectral reflectance (b) for data acquired from boat-mounted spectroradiometer in the La Jolla kelp bed on 23 August 1987.

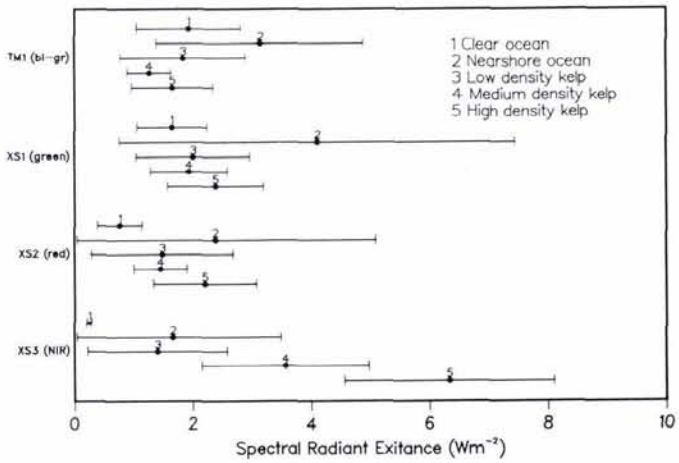

FIG. 3. Coincident spectral plot of spectral radiant exitance (SRE) data acquired from boat. Bars show the mean SRE value in each sample class (center point) plus and minus one standard deviation. Substantial overlap of the bars indicates poor separability between classes.

TABLE 3. SIGNIFICANCE LEVELS FOR T-TESTS OF SPECTRAL RADIANT EXITANCE DATA ACQUIRED FROM BOAT

Class Group	TM1	XS1	XS2	XS3
Clear/Nearshore	—	*	—	*
Clear/Low	—	—	—	*
Clear/Medium	**	—	*	**
Clear/High	—	*	***	***
Nearshore/Low	**	**	—	—
Nearshore/Medium	***	**	—	**
Nearshore/High	***	**	—	***
Low/Medium	*	—	—	***
Low/High	—	—	**	***
Medium/High	**	**	***	***

— not significant
* significant at the 95% level
** significant at the 99% level
*** significant at the 99.99% level

and nearshore ocean waters. To determine whether the SRE values of kelp density and ocean classes were significantly different in each spectral band, the two-group form of the Student's t-test was performed on the means of class pairs (or groups). T-test results shown in Table 3 verify that the NIR band (XS3) was the most effective single band for discrimination of the five classes sampled from boat, as XS3 SRE mean values were significantly different for all class combinations (groups) except nearshore water/low density kelp. Initially it was hypothesized that reflections from subsurface kelp would result in higher SRE and spectral reflectance in the blue-green (TM1) and green (XS1) bands compared to open water with no kelp present (Swain and Davis, 1978). However, the mean SRE values for clear water and low density kelp plots were not significantly different in either of these bands, so the water penetration capabilities of

bands XS1 and TM1 did not appear to be of value for discriminating subsurface kelp.

The mean SRE for each class from the La Jolla sample sites extracted from the two SPOT images is shown graphically in Figure 4, and the brightness value (BV) and SRE data for the 10 October 1987 image are listed in Table 4. This image received primary attention because the canopy extent and development were greater in late 1987 than during acquistion of the 22 November 1986 image.

The green band (XS1) was the most sensitive of the three bands to sea surface roughness and to water turbidity occurring in the nearshore areas. The smoothing effect of the kelp canopy on the water surface reduced sun glint, which resulted in lower band XS1 values in the kelp bed relative to surrounding ocean areas. Figure 5a reveals that the lowest band XS1 BVs occurred in very clear, calm waters in the south central portion of the bed where the canopy had recently been harvested. The red band (XS2), shown in Figure 5b, was not as sensitive to water turbidity as the green band. Red reflectance from kelp was high enough to allow high density and some medium density kelp areas to be identified visually in the band XS2 image, but reflectance differences in the red were not sufficient for discriminating ocean from lower density kelp. Similar BVs for turbid nearshore waters and higher density areas of kelp in the red band are also apparent in Figure 5b. In the NIR band (XS3) image shown in Figure 5c, relatively high reflectance from the kelp canopy and strong absorption by the surrounding water surfaces resulted in highly contrasting spectral signatures between kelp and outer ocean. Low-to-high canopy density gradients were also identified by a corresponding spatial gradient in NIR radiance. Fringe areas of kelp and nearshore waters, however, exhibited similar NIR values.

Brightness values and SRE ranges for the 22 November 1986 SPOT HRV-XS image were generally similar to those of the 10 October 1987 image. Unlike 1987, the kelp bed outline could not be identified in the green band (XS1), probably because high waves and stronger wind speeds caused greater surface roughness within the bed area (see Table 1). As in the 1987 image, band XS2 was only useful for discriminating denser kelp canopy from ocean areas. The 1986 band XS3 shown in Figure 5d provided a high contrast between kelp and ocean. Vertical striping apparent in some areas of Figure 5d was due to pixel values one BV higher relative to surrounding unaffected areas.

The signature overlap between kelp and turbid nearshore ocean areas was reduced for XS3/XS2 and XS3/XS1 band ratio images, while the high discrimination between kelp and open ocean provided by the NIR band was maintained. The XS3/XS2 ratio proved superior to the XS3/XS1 ratio for discriminating kelp from ocean on both image dates. The band ratio images proved to be a simple, effective way to discriminate areas of kelp from most nearshore ocean areas, and provided a useful alternative to more time consuming statistical classification methods for determining the margins between kelp, ocean, and land areas. (Unsupervised clustering of the image data adequately discriminated between most ocean, kelp, and land areas, but failed to distinguish ocean from low density fringe areas of kelp.) The ratio images also served to normalize for differences in irradiance between the two image dates. The primary disadvantage of the XS3/XS2 band ratio technique compared to statistical classification techniques was the need for manual masking of isolated areas of nearshore turbid water that exhibited the same ratio BVs as areas of kelp. The documented water depth ranges for kelp were used as the criteria for manually separating water from kelp in these areas.

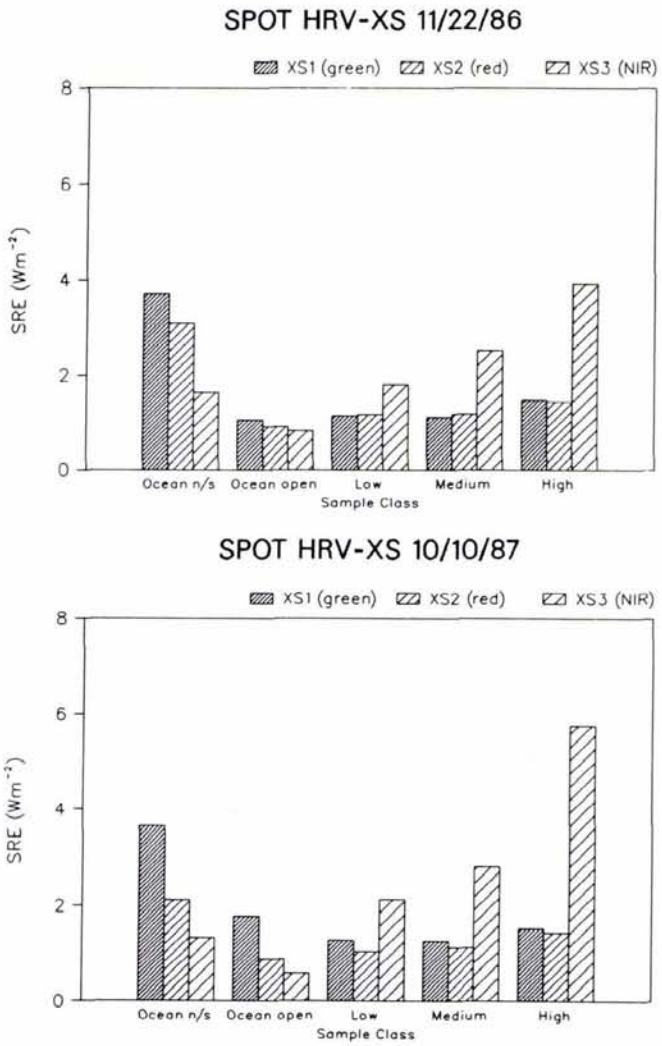

FIG. 4. Mean spectral radiant exitance (SRE) values for ocean and kelp sample classes in sensor bands XS1, XS2, and XS3 for both SPOT images. SRE data were derived from the mean brightness values of sample sites in the La Jolla kelp bed.

TABLE 4. 10 OCTOBER 1987 SPOT HRV-XS BRIGHTNESS VALUE (BV) RANGE, MEAN AND STANDARD DEVIATION, AND MEAN SPECTRAL RADIANT EXITANCE (SRE)

	Band XS1 (green)				Band XS2 (red)				Band XS3 (NIR)			
Class	BV Range	Mean BV	S.D.	Mean SRE	BV Range	Mean BV	S.D.	Mean SRE	BV Range	Mean BV	S.D.	Mean SRE
Nearshore Ocean	7-52	11.19	3.35	3.66	3-47	8.72	3.76	2.13	2-24	3.93	1.96	1.35
Outer Ocean	4-6	5.49	0.37	1.79	1-4	3.64	0.31	0.89	1-3	1.70	0.34	0.58
Low Density	3-5	3.95	0.47	1.29	3-6	4.30	0.54	1.05	4-10	6.20	1.22	2.14
Medium Density	2-5	3.88	0.43	1.27	3-7	4.67	0.81	1.14	4-15	8.14	1.74	2.81
High Density	4-5	4.70	0.40	1.54	3-7	5.93	0.44	1.45	8-22	16.71	2.81	5.77

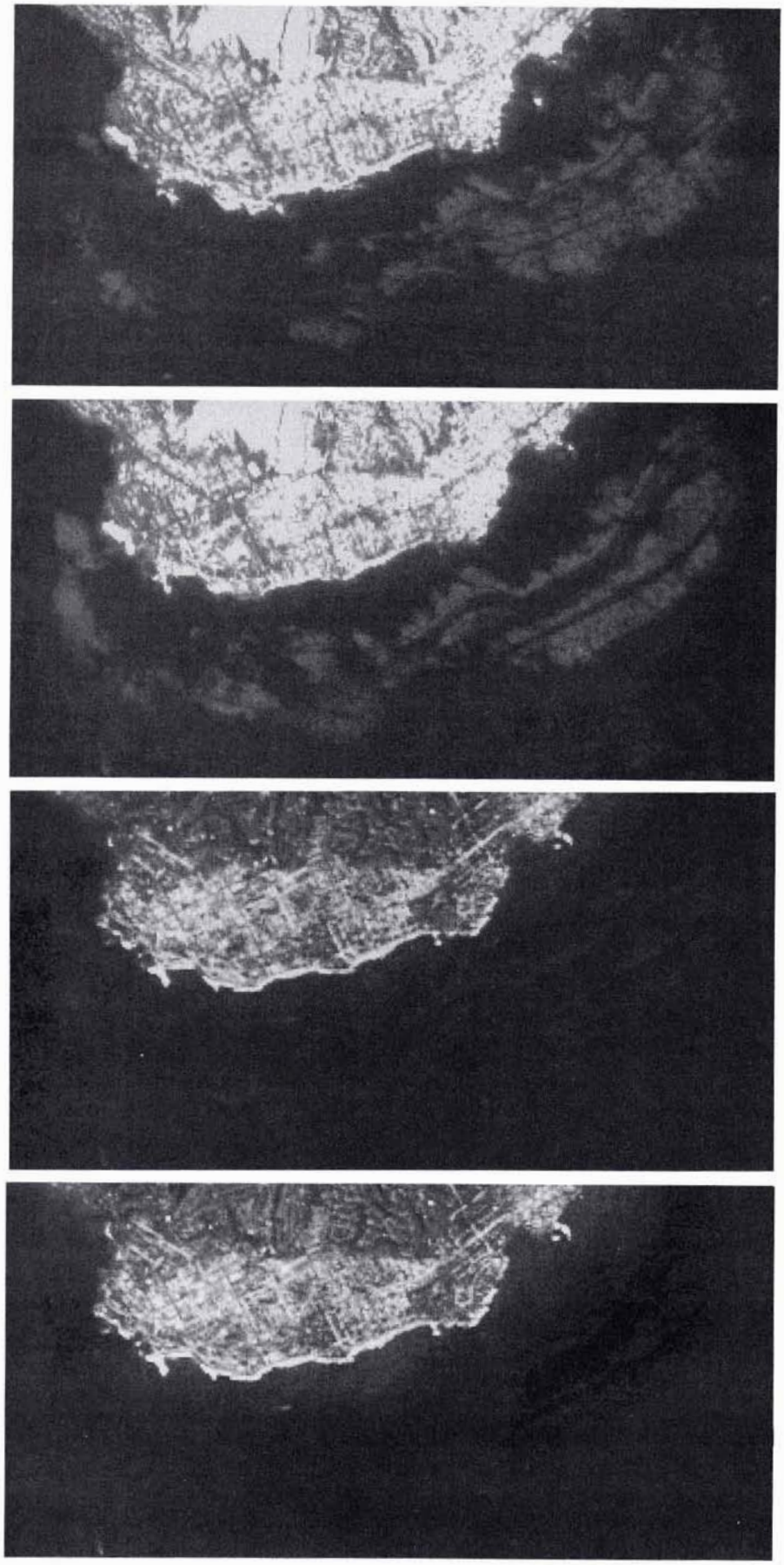

FIG. 5. SPOT HRV-XS La Jolla subscenes: (a) 1987 band XS1 (green); (b) 1987 band XS2 (red); (c) 1987 band XS3 (NIR); (d) 1986 band XS3 (Copyright SPOT Image Corp, 1986 and 1987). All bands were histogram-equalized to improve contrast.

All four spectral vegetation indices (SVI) analyzed (SR, NDVI, TVI, and NIR/Green) were found to be sensitive to variations in kelp canopy density. The SVI values shown in Table 5 derived from both the SPOT and boat SRE data sets corresponded to the relative density of kelp when differences in sampling methodologies were taken into consideration. The primary differences were that boat samples visually classified as low density were composed primarily of subsurface kelp, while the low density sample sites on the SPOT scenes were categorized according to surface canopy identifiable on maps derived from aerial photographs. Red SRE often exceeded NIR SRE in the subsurface kelp areas (due to NIR absorption by water), which resulted in lower SVI values in general and negative NDVI values.

One of the reasons for using an SVI was to normalize image data for differences in illumination conditions. Using SVIs, therefore, more reliable comparisons could be made between the SPOT and boat data sets, and the multi-date SPOT images, than could be made from the NIR band SRE data alone. The development of the three NIR to red band SVIs used in this study was based on the reflectance properties of terrestrial vegetation, whose absorption of red wavelength light by chlorophyll and other photosynthetic pigments causes a decrease in red radiance as biomass density increases. In contrast, the red radiance values in the kelp canopy tended to increase in proportion to canopy density because the pigmentation of *M. pyrifera* (a brown algae) does not exhibit the photosynthetic absorption characteristics common in "green" vegetation.

Spatial Aspects of the Kelp Bed Environment

The smallest patches of kelp identifiable on 1:40,000-scale CIR aerial photographs were measured to be approximately one metre in diameter. Comparative analysis of CIR aerial photographs and the band XS3 image data showed that the SPOT HRV sensor was able to detect kelp from an ocean background when the canopy coverage of dense kelp within a pixel was at least 25 m^2 in area. This meant that approximately 6 percent of a SPOT HRV-XS pixel must have been comprised of dense kelp canopy in order to boost the radiometric response in the NIR band one brightness value above the noise level. Thus, the sensor's NIR radiometric resolution was capable of discriminating relatively small patches of dense kelp. An increase in the percentage (or coverage) of surface canopy within a pixel resulted in a corresponding increase in radiance detectable by the sensor. However, a pixel containing a small patch of high density canopy could produce the same NIR response as one that was primarily filled with low density partially submerged kelp.

TABLE 5. MEAN SPECTRAL VEGETATION INDEX VALUES FOR KELP CLASSES USING SPECTRAL RADIANT EXITANCE DATA ACQUIRED FROM BOAT AND SPOT PLATFORMS

Boat (23 Aug 87) Class	XS3/XS2	XS3/XS1	NDVI	TVI
Low	0.856	0.660	−0.160	0.532
Medium	2.246	1.708	0.278	0.866
High	3.280	2.862	0.486	0.986
SPOT (22 Nov 86) Class	**XS3/XS2**	**XS3/XS1**	**NDVI**	**TVI**
Low	1.771	1.987	0.268	0.875
Medium	2.161	2.484	0.354	0.922
High	3.136	3.648	0.505	1.001
SPOT (10 Oct 87) Class	**XS3/XS2**	**XS3/XS1**	**NDVI**	**TVI**
Low	1.647	1.284	0.233	0.854
Medium	2.495	2.147	0.408	0.951
High	3.748	3.600	0.572	1.035

Estimates of kelp canopy areal extent derived from SPOT digital data are compared with estimates derived from CIR aerial photographs (W. North, unpublished maps, 1986-1987) in Table 6. An estimate for the Point Loma bed in 1987 derived from CIR aerial photographs by the Kelco Division of Merck and Co, Inc. (D. Glantz, personal communication, 1989) is also included in Table 6. The SPOT-derived estimates were two to three times higher than those derived by North from aerial photographs, probably due to differences in the approach used to make each estimate. The grid count method (Maling, 1989) used by North to estimate kelp area from the aerial photographs accounted for many small pockets of open water within the kelp bed. Areas of patchy kelp and pockets of water may have been mapped as 100 percent kelp by SPOT due to its lower spatial resolution and the integrating nature of a pixel.

Although the SPOT data yielded less detailed maps that primarily identify canopy boundaries (apparent in Figure 6), this degree of accuracy was deemed appropriate for most resource management applications (W. North, personal communication, 1989). In addition, the SPOT-derived estimate for Point Loma was within 4 percent of Kelco's estimate, which was derived by planimeter (the most commonly used method for deriving kelp extent from aerial photographs). The planimeter method tends to produce higher estimates because it traces the general boundaries of canopy areas and does not account for small gaps within the canopy (D. Glantz, personal communication, 1989). Kelp harvesting and differences in tide height between dates also account for some portion of the differences between estimates, although the exact contribution could not be determined. Substantial harvesting of the canopy occurred between the SPOT and aerial photograph acquisition dates. Higher tide heights during both SPOT acquisitions (see Table 1) may have submerged a greater portion of the canopy (McFarland and Prescott, 1959), and the kelp bed aerial photographs were acquired near peak low tide.

Of primary importance for areal extent estimates is the relative accuracy of the estimates from date to date. The substantial difference in the Point Loma 1987 estimates made by North and Kelco was not uncommon (D. Glantz, personal communication, 1989). Another study compared aerial photograph-based estimates for several beds made by three independent sources and also found wide variations in areal extent estimates (N. M. I., 1981). Consecutive manually derived estimates with both the grid count and planimeter methods routinely vary by 10 to 20 percent (W. North and D. Glantz, personal communications, 1989). It was not possible to determine if the SPOT-derived estimates were any more accurate in an absolute sense than the manually derived estimates. However, the fact that the SPOT estimates were derived using more consistent and repeatable methods means that date-to-date comparisons would produce more accurate quantifications of kelp bed areal extent changes.

In overall size, kelp beds are relatively small features on a regional scale (ranging from thousands of square metres to sev-

TABLE 6. KELP BED AREAL EXTENT ESTIMATES DERIVED FROM DIGITAL SPOT IMAGE DATA AND CIR AERIAL PHOTOGRAPHS

Source	Date	Location	Area Extent m^2
SPOT HRV-XS	22 Nov 86	La Jolla	3,573,600
North CIR	10 Dec 86	La Jolla	930,000
SPOT HRV-XS	10 Oct 87	La Jolla	4,610,800
North CIR	10 Sep 87	La Jolla	2,370,000
SPOT HRV-XS	10 Oct 87	Point Loma	7,047,600
North CIR	15 Jun 87	Point Loma	3,680,000
Kelco CIR	22 Jul 87	Point Loma	7,282,800

eral square kilometres). Therefore, the acquisition of satellite data solely for the purpose of mapping such small areas may be cost prohibitive. Because large kelp beds are typically long, narrow features, image acquisitions from aircraft with pushbroom radiometers similar to the SPOT HRV could prove to be more cost effective for acquiring data on kelp beds. Satellite data may prove more cost effective for larger scale applications such as inventories of open ocean kelp farms proposed for the future (Neushul, 1980), or when the image data are also used for other coastal zone applications.

Map Analysis

Kelp distributions during the 1987 time period derived from CIR aerial photographs (W. North, unpublished map, 1987) are compared with distributions derived from the XS3/XS2 band ratio of the SPOT digital data in Figure 6. Grey scales were selected for the SPOT-derived map to indicate relative density (darkest being the most dense surface canopy). The extent of kelp is depicted similarly on both maps, although the SPOT-derived map does not show some small isolated patches that were identified on aerial photographs. Swaths cut through the canopy by kelp harvesters between the dates of the aerial photograph and SPOT acquisitions are clearly visible on the SPOT-derived map. In addition, density patterns indicated on the SPOT-derived map (based on differences in NIR radiance) closely correspond to density patterns indicated by canopy spacing on the aerial photograph-derived map.

Figure 7 is a canopy density map based on an XS3/XS2 (NIR/red) band ratio of the 10 October 1987 SPOT HRV-XS data (kelp density class thresholds were derived as described previously in "Methodology"). This type of thematic map is useful for those who harvest and monitor the resource because it provides information on both canopy extent and relative density throughout the bed. Many of the change detection methods tested produced maps that grouped ocean and kelp change areas together. The best results were obtained using the matrix analysis technique (Figure 8). The change map in Figure 8 clearly delineates areas (or "zones") of change between the two dates (approximately 11 months apart). Dramatic regeneration of the canopy is evident in the northern portion of the bed due to favorable growing conditions for kelp during 1987.

CONCLUSIONS

Multispectral digital data acquired by the SPOT HRV sensor was processed to yield kelp information that met or exceeded present monitoring requirements for kelp distribution mapping and quantification of areal extent. SPOT HRV band XS3 (NIR) provided high contrast between kelp and the ocean background, and NIR radiance increased as a function of increasing canopy density. Band XS3 thus yielded the most information for detecting kelp surface canopy and for identifying relative densities in canopy coverage. Although bands XS2 (red) and XS1 (green) were marginally useful for discriminating kelp from open water, these bands were most useful for minimizing confusion between kelp and turbid water that can occur in the NIR band, and for normalizing the NIR data for multi-date comparisons. The water penetration capabilities of bands XS1 and XS2 did not prove to be of value for discrimination of subsurface kelp.

Areal extent estimates derived from SPOT HRV data were higher than those derived manually by the grid count method from aerial photographs, but a SPOT estimate was very close to one derived by a commercial firm using polar planimeter area measurement. The SPOT-based estimates were also derived in a more

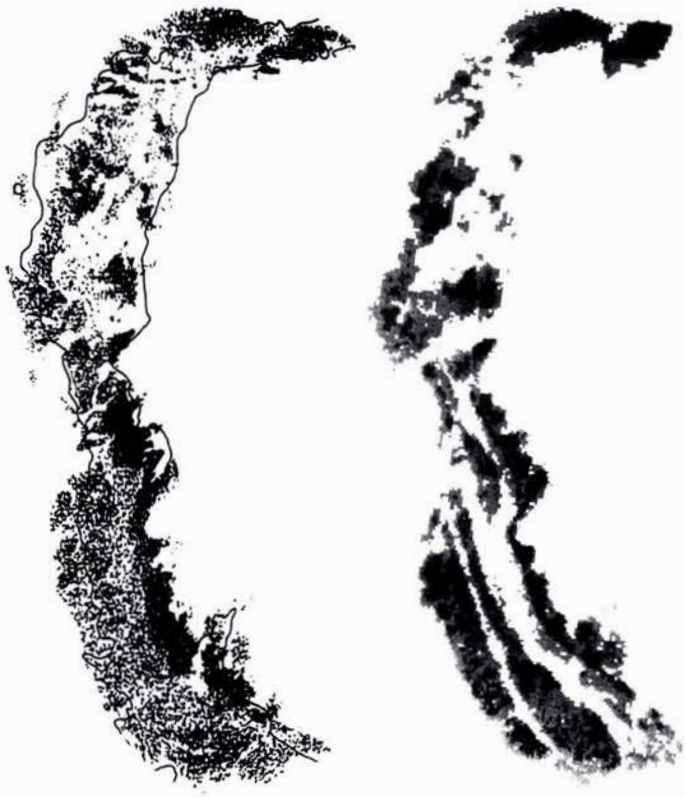

FIG. 6. Comparison of La Jolla kelp distributions during fall 1987 derived from CIR aerial photographs and SPOT HRV-XS digital data. Figure 6a was manually traced from CIR aerial photographs taken on 10 September 1987 (W. North, unpublished map, 1987). Figure 6b was derived from an XS3/XS2 band ratio of the SPOT digital data acquired on 10 October 1987. Absence of canopy in the central area of Figure 6b is primarily due to kelp harvesting between dates.

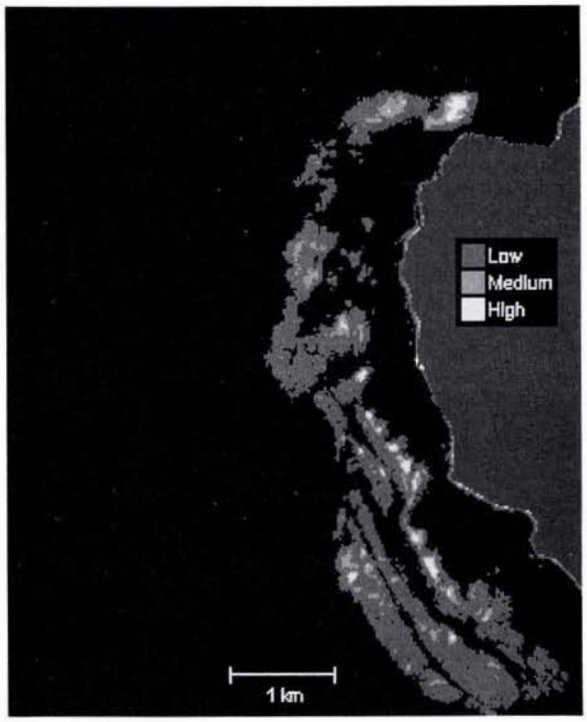

FIG. 7. Kelp distribution and density map of the La Jolla bed derived from an XS3/XS2 (NIR/red) band ratio of the 10 October 1987 SPOT digital data. The kelp canopy had been recently harvested in high density areas in the central portion of the bed.

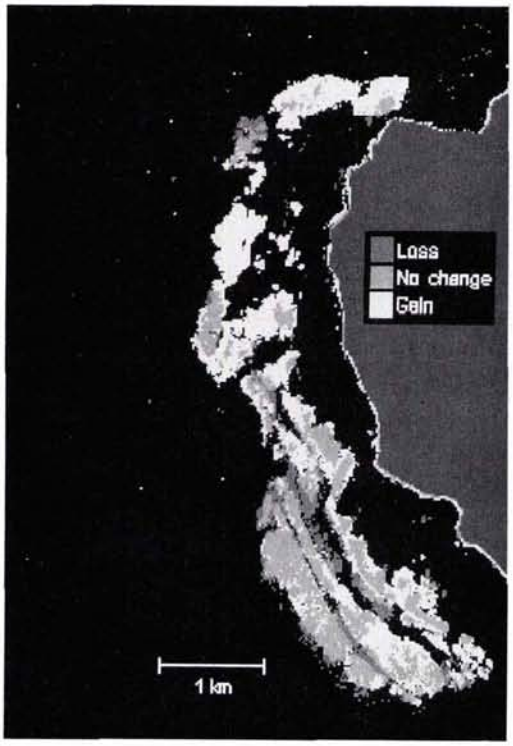

FIG. 8. Canopy change map of the La Jolla bed between 22 November 1986 and 10 October 1987 derived using matrix analysis (Jensen, 1986). Dramatic regeneration of the canopy is evident in the northern half of the bed, and small areas of loss in the central portion are due to harvesting prior to the 1987 image acquistion.

consistent repeatable manner, thus minimizing the interpreter error common in manual techniques and allowing more confident date-to-date comparisons.

Image processing techniques allowed relatively easy production of thematic maps of canopy density and canopy change that were produced subjectively and with more difficulty using manual techniques based on aerial photographs. The digital format of satellite data would also allow for easy integration of kelp distribution and density data into a GIS database of water quality and bathymetric parameters in a manner similar to that described by Welch *et al.* (1988). The acquisition of satellite data solely for mapping kelp beds may prove cost prohibitive unless the imagery were utilized for additional applications or acquired for surveying kelp over large areas of coastline.

ACKNOWLEGMENTS

Dr. Wheeler J. North of the California Institute of Technology in Pasadena and Ron McPeak and Dale Glantz of the Kelco Division of Merck and Company, Inc. in San Diego provided kelp maps, areal extent estimates, and information on the biological and historical aspects of kelp populations. David McKinsey (SDSU) assisted with image processing tasks, and Blake H. Burns (SDSU) helped with the acquisition and processing of the *in situ* radiometer data. Dr. John R. Jensen (University of South Carolina) helped to initiate and develop the scope of this project.

REFERENCES

Austin, A., and R. Adams, 1978. Aerial Color and Color Infrared Survey of Marine Plant Resources, *Photogrammetric Engineering & Remote Sensing*. 44:469–480.

Jensen, J. R., 1986. *Introductory Digital Image Processing: A Remote Sensing Perspective*, Prentice-Hall, Englewood Cliffs, N.J.

Jensen, J. R., L. Tinney, and J. Estes, 1976. Maximum Likelihood Classification of Kelp Resources (*Macrocystis pyrifera*) from Landsat Computer Compatible Tapes, *Proceedings of the Second Annual William T. Pecora Symposium*, American Society of Photogrammetry, pp. 201–212.

———, 1980. Remote Sensing Techniques for Kelp Surveys, *Photogrammetric Engineering & Remote Sensing*. 46:743–755.

Jensen, J. R., J. Estes, and J. Scepan, 1987. Monitoring Changes in Giant Kelp Distribution Using Digital Remote Sensor Data, *Photo Interprétation*. 87–1:25–29.

Maling, D. H., 1989. *Measurements from Maps: Principles and Methods of Cartometry*, Pergamon Press, New York.

McFarland, W., and J. Prescott, 1959. *Standing Crop, Chlorophyll Content and In Situ Metabolism of a Giant Kelp Community in Southern California*. Institute of Marine Science, University of Texas. 6:109–132.

McPeak, R. H., and D. Glantz, 1984. Harvesting California's Kelp Forests, *Oceanus*. 27:19–26.

Mel, M., 1977. *Aerial Remote Sensing of Subtidal Vegetation in Southern California*, Master's Thesis, University of California at Los Angeles.

Neushul, M., 1980. *Energy from Open Ocean Kelp Farms*, Report to the Committee on Commerce, Science, and Transportation, Washington, D. C., n.p.

N. M. I., 1981. *Historical Review of Kelp Beds in the Southern California Bight*, Southern California Edison Research Report Series Number 81-RD-98, Neushul Mariculture Inc., Goleta, Calif.

North, W. J., (ed.), 1971. *The Biology of Giant Kelp Beds (Macrocystis) in California*, Nova Hedwigia, Heft 32.

Singh, A., 1985. Thematic Mapper Radiometric Correction Research and Development Results and Performance, *Photogrammetric Engineering & Remote Sensing*. 51:1379–83.

SPOT Image Corporation, 1989. *SPOT Image Handbook*, SPOT Image Corporation, Reston, Virginia.

Swain, P. H., and S. M. Davis (eds.), 1978. *Remote Sensing: The Quantitative Approach*, McGraw-Hill, New York.

Welch, R., M. M. Remillard, and R. B. Slack, 1988. Remote Sensing and Geographic Information System Techniques for Aquatic Resource Evaluation, *Photogrammetric Engineering & Remote Sensing*. 54:177–85.

(Received 2 April 1990; accepted 2 July 1990; revised 12 September 1990)